



Published in final edited form as:

Nature. 2009 May 21; 459(7245): 428–432. doi:10.1038/nature08012.

Non-genetic origins of cell-to-cell variability in TRAIL-induced apoptosis

Sabrina L. Spencer^{1,2,*}, Suzanne Gaudet^{1,3,*}, John G. Albeck¹, John M. Burke¹, and Peter K. Sorger¹

¹Center for Cell Decision Processes, Department of Systems Biology, Harvard Medical School, MA 02115

²Computational and Systems Biology, Massachusetts Institute of Technology, Cambridge, MA 02139

Abstract

In microorganisms, noise in gene expression gives rise to cell-to-cell variability in protein concentrations^{1–7}. In mammalian cells, protein levels also vary^{8–10} and individual cells differ widely in responsiveness to uniform physiological stimuli^{11–15}. In the case of apoptosis mediated by TRAIL (TNF related apoptosis-inducing ligand) it is common for some cells in a clonal population to die while others survive – a striking divergence in cell fate. Among cells that die, the time between TRAIL exposure and caspase activation is highly variable. Here we image sister cells expressing reporters of caspase activation and mitochondrial outer membrane permeabilisation (MOMP) following exposure to TRAIL. We show that naturally occurring differences in the levels or states of proteins regulating receptor-mediated apoptosis are the primary causes of cell-to-cell variability in the timing and probability of death. Protein state is transmitted from mother to daughter, giving rise to transient heritability in fate, but protein synthesis promotes rapid divergence so that sister cells soon become no more similar to each other than pairs of cells chosen at random. Our results have implications for understanding “fractional killing” of tumor cells following exposure to chemotherapy, and for variability in mammalian signal transduction in general.

TRAIL elicits a heterogeneous phenotypic response in both sensitive and relatively resistant cell lines: some cells die within 45 min, others 8–12 hr later, and yet others live indefinitely (Supplementary Fig. 1). During the variable delay between TRAIL addition and MOMP, upstream initiator caspases are active but downstream effector caspases are not^{11,12}. Possible sources of cell-to-cell variability in responses to TRAIL include genetic or epigenetic differences, stochastic fluctuations in biochemical reactions involving low copy number components (“intrinsic noise”³), differences in cell cycle phase, and natural

Users may view, print, copy, and download text and data-mine the content in such documents, for the purposes of academic research, subject always to the full Conditions of use:http://www.nature.com/authors/editorial_policies/license.html#terms

[†]Please address correspondence to: Peter K. Sorger, Department of Systems Biology, WAB Room 438, Harvard Medical School, 200 Longwood Avenue, Boston, MA 02115, (peter_sorger@hms.harvard.edu).

^{*}These authors contributed equally to this work

³Current address: Department of Cancer Biology, Dana-Farber Cancer Institute, and Department of Genetics, Harvard Medical School, Boston, MA 02115

variation in the concentrations of key reactants. To distinguish among these and other possibilities, we used live-cell microscopy to compare the timing and probability of death in sister cells exposed to TRAIL. Were phenotypic variability caused by genetic or epigenetic differences, sister cells should behave identically. In contrast, were stochastic fluctuations in reactions triggered by TRAIL to predominate, sister cells should be no more similar to each other than pairs of cells selected at random. The influence of cell cycle state on apoptosis should be readily observable from time-lapse imaging of asynchronous cultures. Finally, variability arising from differences in protein levels (or in activity or modification state) should produce a highly distinctive form of inheritance in which newly born sister cells are very similar, because they inherit similar numbers of abundant factors from their mother^{4,7}, but then diverge as new proteins are made and levels drift^{10,16}. With this in mind, we examined apoptosis in HeLa cells and in non-transformed MCF10A mammary epithelial cells in the presence and absence of protein synthesis inhibitors.

Pairs of sister cells expressing a fluorescent reporter of MOMP (IMS-RP11) born during a 20–30 hr period were identified by time-lapse microscopy. TRAIL and the protein synthesis inhibitor cycloheximide were then added and filming continued for another 8 hr. The TRAIL to MOMP interval (T_d) was calculated for each cell (Fig. 1a). Among recently divided sisters (< 7 hr between division and death), T_d was highly correlated ($R^2 = 0.93$, Fig. 1b) whereas T_d was uncorrelated ($R^2 = 0.04$) for recently divided cells chosen at random. Time since division (Fig. 1c) and position in the dish (data not shown) did not correlate with T_d , ruling out a role for cycle state and cell-cell interactions under our experimental conditions. However, as time since division increased, sister-to-sister correlation in T_d decayed exponentially with a half-life of ~11 hr so that sisters lost memory of shared ancestry within 50 hours or about 2 cell generations ($R^2 = 0.05$, the same as random pairs of cells; Fig. 1d,e). Similar results were obtained with MCF10A cells (Supplementary Fig. 2).

High correlation among recently born sisters shows that variability in T_d arises from differences that exist prior to TRAIL exposure and rules out stochastic fluctuations in signaling reactions. Rapid decorrelation also rules out genetic mutation or conventional epigenetic differences (which typically last 10–10⁵ cell divisions¹⁷). However, transient heritability is precisely what we expected for cell-to-cell differences arising from variations in the concentrations or states of proteins that are partitioned binomially at cell division.

Whereas all TRAIL-treated HeLa cells eventually died in the presence of cycloheximide, in its absence a fraction always survived (presumably due to induction of survival pathways¹⁸). When the fates of sister cells were compared, both lived or both died in almost all cases (chi-square test, $p=7\times 10^{-19}$, Supplementary Fig. 3). Variability in T_d across the population was large (Fig. 1g and Supplementary Fig. 4), but recently born sisters were nevertheless correlated in T_d ($R^2=0.75$, Fig. 1f). Again, cell cycle phase was not correlated with fate or time-to-death (Fig. 1g). Decorrelation in T_d among sisters was an order of magnitude more rapid in the presence of protein synthesis than in its absence (~1.5 hr half-life, Fig. 1h,i and Supplementary Fig. 5). Thus, the length of time that T_d is heritable is very sensitive to rates of protein synthesis, both basal and TRAIL-induced.

Are the concentrations of proteins regulating TRAIL-induced apoptosis sufficiently different from cell to cell to account for variability in T_d ? Using flow cytometry, we measured the distributions of five apoptotic regulators for which specific antibodies are available. All five proteins were log-normally distributed across the population with coefficients of variation between 0.21 and 0.28 for cells of similar size (Fig. 2a), consistent with data on other proteins¹⁰. To determine the impact of variability in protein levels on variability in time-to-death, we turned to an ordinary differential equation model of TRAIL-induced apoptosis¹². This model encapsulates the biochemistry of TRAIL-mediated death and recapitulates the dynamics of apoptosis under various conditions of protein depletion or over-expression¹². When variability in T_d arising from variance in protein levels was modeled, a good match was observed to experimental data (Fig. 2b–d) implying that measured differences in protein levels are sufficient to account for variability in T_d .

Which steps in receptor-mediated apoptosis are responsible for variation in time-to-death? To address this question, we grouped reactions into three sets: those occurring before, during, or subsequent to MOMP (Fig. 3a – blue, grey, and orange). Before MOMP, TRAIL binds and oligomerizes DR4/5 receptors, promoting assembly of death-inducing signaling complexes (DISCs) that then activate initiator pro-caspases-8 and -10 (C8/10)¹⁹. Active C8/10 cleaves Bid to tBid^{20,21}, which activates the pore-forming proteins Bax and Bak²². C8/10 also processes effector pro-caspases-3 and -7 (C3/7) but C3/7 activity is held in check by XIAP until MOMP¹⁹. MOMP itself involves self-assembly of activated Bax/Bak into transmembrane pores, a process antagonized by anti-apoptotic Bcl-2 proteins²². When levels of activated tBid, Bax, and Bak exceed a threshold set by inhibitory Bcl-2 proteins, pores form in the mitochondrial outer membrane, allowing cytochrome *c* and Smac to translocate into the cytosol²². In post-MOMP reactions, cytosolic Smac neutralizes XIAP, relieving C3/7 inhibition and allowing cleavage of effector caspase substrates and consequent cell death¹⁹. In a parallel route to C3/C7 activation, cytosolic cytochrome *c* promotes apoptosome assembly and caspase-9 activation.

To determine which steps in TRAIL-induced apoptosis play the greatest role in determining variability in death time, we imaged cells expressing a reporter of either initiator or effector caspase activity (IC-RP or EC-RP)¹¹ in combination with IMS-RP. We found almost all variability in T_d to arise during the pre-MOMP interval (Fig. 3b). The timing of MOMP itself is determined by the rate at which tBid accumulates to a threshold set by the levels of Bcl-2 family proteins. This rate and threshold can be determined from the initial rate of IC-RP cleavage (k_{IC}) and the fraction of IC-RP cleaved (θ) at the time of MOMP, respectively. When k_{IC} and θ were measured in single TRAIL-treated cells, the timing of MOMP was found to be controlled by a variable rate of approach to a threshold of variable height (Fig. 3c,d). However, variation in k_{IC} played a significantly greater role in determining T_d than variation in θ ($R^2=0.82$ vs. $R^2=0.22$; Fig. 3e,f, and Supplementary Fig. 7). Moreover, k_{IC} was very similar in recently born sister cells with similar T_d , but dissimilar in older sisters (Fig. 3g). We conclude that cell-to-cell variability in k_{IC} – and by implication the rate of conversion of Bid to tBid – is the primary determinant of variability in time-to-death under our experimental conditions.

Levels of multiple proteins set k_{IC} , including DR4/5 receptors, DISC components, C8, and Bid itself. Modelling suggested that knowing the concentration of any single protein upstream of Bid would have minimal value in predicting T_d – the impact of variation in all other proteins is too great (Fig. 4a). Live-cell analysis of FLIP, an important regulator of pro-caspase-8 binding to the DISC, was consistent with this prediction, as was analysis of other single proteins by flow cytometry (Fig. 4b and data not shown). However, modelling showed that with increasing over-production of Bid, measurement of its levels would be increasingly predictive of T_d (Fig. 4c, Supplementary Fig. 8). We therefore measured the relationship between dispersion in T_d and levels of Bid-GFP (Fig. 4d). A ~50-fold increase in Bid-GFP caused the variability in T_d to fall significantly, concomitant with a decrease in mean time-to-death from ~3 hr to ~45 min. Thus, only when over-expressed is the level of one protein predictive of T_d ; under normal circumstances, control is multivariate.

Other studies (for example, ref. 23) address genetic factors determining the average sensitivity of cell lines to TRAIL whereas this paper examines non-genetic cell-to-cell variability within an individual cell line. We come to three primary conclusions. First, cell-to-cell variation in the timing and probability of death is transiently heritable. Cell cycle state, number of neighbouring cells, and stochastic fluctuations in TRAIL-induced signalling reactions do not play a major role under our conditions. Instead, variability in phenotype arises from cell-to-cell differences in protein levels that exist prior to TRAIL exposure (our experiments do not distinguish between cell-to-cell differences in total concentrations or in post-translationally modified forms). Second, the rate at which sisters lose memory of a shared past is an order of magnitude faster in the presence of protein translation than in its absence. This further implicates variability in protein levels as the origin of differences in phenotype. Third, knowing the concentration of individual proteins does not allow T_d to be predicted but measuring the rate of a single reaction does (Bid to tBid conversion in our experiments). These findings are likely to hold for other examples of ligand-induced apoptosis, however for intrinsic apoptosis, different proteins will control the rate of approach to MOMP and θ may dominate in certain contexts. Moreover, given the prevalence of multi-protein cascades in signal transduction, multivariate control over cell-to-cell variability is likely to be more common than the univariate control observed in other settings^{8,23,24}.

Heritable, non-genetic determinants of phenotype are often referred to as “epigenetic”¹⁷, but the transient heritability we observe is fundamentally different in origin and duration. Given variability in growth rates and noise in gene expression, genetically identical cells will inevitably contain slightly different concentrations of most proteins. However, differences in protein concentrations do not necessarily affect phenotype, a property often referred to as robustness²⁵. For example, the efficiency with which effector caspase substrates are cleaved does not vary from cell to cell¹¹. Given the importance of tight control over apoptosis, cell-to-cell variability in the timing and probability of death seems unlikely to reflect an inability of cells to achieve robust regulation. Instead, by transforming what is a binary decision at the single-cell level into a graded response at the population level, variability probably has an adaptive advantage. TRAIL is currently undergoing clinical trials as an anti-cancer drug²⁶ and our findings may have implications for the use of TRAIL and other apoptosis

inducers as therapeutics. Many drugs exhibit “fractional killing” in which each round of therapy kills some but not all of the cells in a tumor²⁷. Traditionally, this is thought to reflect differences in genotype, cell cycle state, or the involvement of cancer stem cells, but our data demonstrate that dramatic variability can also arise from natural differences in protein levels. We propose that the efficiency of TRAIL-mediated killing of cancer cells could be increased by reducing the impact of cell-to-cell variability, perhaps through co-drugging.

Methods Summary

Live-cell microscopy

Cells expressing IMS-RP and FRET reporters EC-RP or IC-RP were imaged as described¹¹. In Figure 1, cells were imaged for 20–30hr to determine time of division and identify sisters; then media containing 50 ng/ml TRAIL plus 2.5 µg/ml cycloheximide or 250 ng/ml TRAIL alone was added. The difference in TRAIL concentrations was designed to generate a similar range in T_d with and without cycloheximide (Supplementary Fig. 4). Cells were then imaged for 8 hr to determine the time of MOMP, by monitoring cytosolic translocation of IMS-RP. Unless otherwise noted, all treatments included 2.5 µg/ml cycloheximide.

Data analysis

Correlation coefficients (R^2) were obtained by linear regression except where noted. Sister-sister correlation was determined by sorting pairs of cells on $T(Div \rightarrow MOMP)_{avg}$ and calculating R^2 for the first 40 pairs. R^2 was then re-calculated for cells 2–41, 3–42, etc., and the results plotted as a function of the average $T(Div \rightarrow MOMP)_{avg}$ for the 40 cells in question, denoted by “ $\langle \rangle$ ”. The results were fit to an exponential decay: $R^2 = 1.2e^{(-0.063T(Div \rightarrow MOMP)_{avg})}$ for TRAIL plus cycloheximide, and $R^2 = 2.3e^{(-0.47T(Div \rightarrow MOMP)_{avg})}$ for TRAIL alone. Half-lives were calculated as $\ln(2)/0.063 = 11$ hr, and $\ln(2)/0.47 = 1.5$ hr. Contributions to T_d of k_{IC} , θ , and pre- and post-MOMP intervals were obtained by fixing one parameter and allowing the other to vary over the observed range, then mean-centring the resulting distributions (Supplementary Fig. 7). Fitted IC-RP trajectories were obtained after subtracting a trajectory for cycloheximide alone (Fig. 3c) to control for photobleaching (Supplementary Fig. 6).

Modelling

The responses of cell populations were simulated using a trained ODE model¹² sampling from log-normally distributed protein concentrations with $CV \approx 0.25$ (see Supplemental Methods). In Figure 4, GFP-Bid (an experimental observable) was added to log-normally distributed endogenous Bid (unobservable); other proteins were sampled from lognormal distributions as before. Simulations were adjusted to match the distribution GFP-Bid achieved experimentally.

Supplementary Material

Refer to Web version on PubMed Central for supplementary material.

Acknowledgements

We thank D. Flusberg, S. Govind, L. Kleiman, A. Letai, B. Millard, R. Milo, T. Norman, J. Paulsson, and R. Ward for their help. This work was supported by NIH grants GM68762 and CA112967.

References

1. Blake WJ, Aern M K, Cantor CR, et al. *Nature*. 2003; 422(6932):633. [PubMed: 12687005]
2. Colman-Lerner A, Gordon A, Serra E, et al. *Nature*. 2005; 437(7059):699. [PubMed: 16170311]
3. Elowitz MB, Levine AJ, Siggia ED, et al. *Science (New York, N.Y.)*. 2002; 297(5584):1183.
4. Golding I, Paulsson J, Zawilski SM, et al. *Cell*. 2005; 123(6):1025. [PubMed: 16360033]
5. McAdams HH, Arkin A. *Proceedings of the National Academy of Sciences of the United States of America*. 1997; 94(3):814. [PubMed: 9023339]
6. Ozbudak EM, Thattai M, Kurtser I, et al. *Nat Genet*. 2002; 31(1):69. [PubMed: 11967532]
7. Rosenfeld N, Young JW, Alon U, et al. *Science (New York, N.Y.)*. 2005; 307(5717):1962.
8. Chang HH, Hemberg M, Barahona M, et al. *Nature*. 2008; 453(7194):544. [PubMed: 18497826]
9. Feinerman O, Veiga J, Dorfman JR, et al. *Science (New York, N.Y.)*. 2008; 321(5892):1081.
10. Sigal A, Milo R, Cohen A, et al. *Nature*. 2006; 444(7119):643. [PubMed: 17122776]
11. Albeck JG, Burke JM, Aldridge BB, et al. *Mol Cell*. 2008; 30(1):11. [PubMed: 18406323]
12. Albeck JG, Burke JM, Spencer SL, et al. *PLoS Biol*. 2008; 6(12):2831. [PubMed: 19053173]
13. Geva-Zatorsky N, Rosenfeld N, Itzkovitz S, et al. *Mol Syst Biol*. 2006; 2 2006 0033.
14. Goldstein JC, Kluck RM, Green DR. *Ann N Y Acad Sci*. 2000; 926:132. [PubMed: 11193030]
15. Lahav G, Rosenfeld N, Sigal A, et al. *Nat Genet*. 2004; 36(2):147. [PubMed: 14730303]
16. Kaufmann BB, Yang Q, Mettetal JT, et al. *PLoS Biol*. 2007; 5(9):e239. [PubMed: 17803359]
17. Rando OJ, Verstrepen KJ. *Cell*. 2007; 128(4):655. [PubMed: 17320504]
18. Chaudhary PM, Eby M, Jasmin A, et al. *Immunity*. 1997; 7(6):821. [PubMed: 9430227]
19. Fuentes-Prior P, Salvesen GS. *Biochem J*. 2004; 384(Pt 2):201. [PubMed: 15450003]
20. Li H, Zhu H, Xu CJ, et al. *Cell*. 1998; 94(4):491. [PubMed: 9727492]
21. Luo X, Budihardjo I, Zou H, et al. *Cell*. 1998; 94(4):481. [PubMed: 9727491]
22. Youle RJ, Strasser A. *Nat Rev Mol Cell Biol*. 2008; 9(1):47. [PubMed: 18097445]
23. Wagner KW, Punnoose EA, Januario T, et al. *Nature medicine*. 2007; 13(9):1070.
24. Cohen AA, Geva-Zatorsky N, Eden E, et al. *Science (New York, N.Y.)*. 2008; 322(5907):1511.
25. Barkai N, Leibler S. *Nature*. 1997; 387(6636):913. [PubMed: 9202124]
26. Ashkenazi A, Herbst RS. *J Clin Invest*. 2008; 118(6):1979. [PubMed: 18523647]
27. Berenbaum MC. *Cancer Chemother Rep*. 1972; 56(5):563. [PubMed: 4652587]

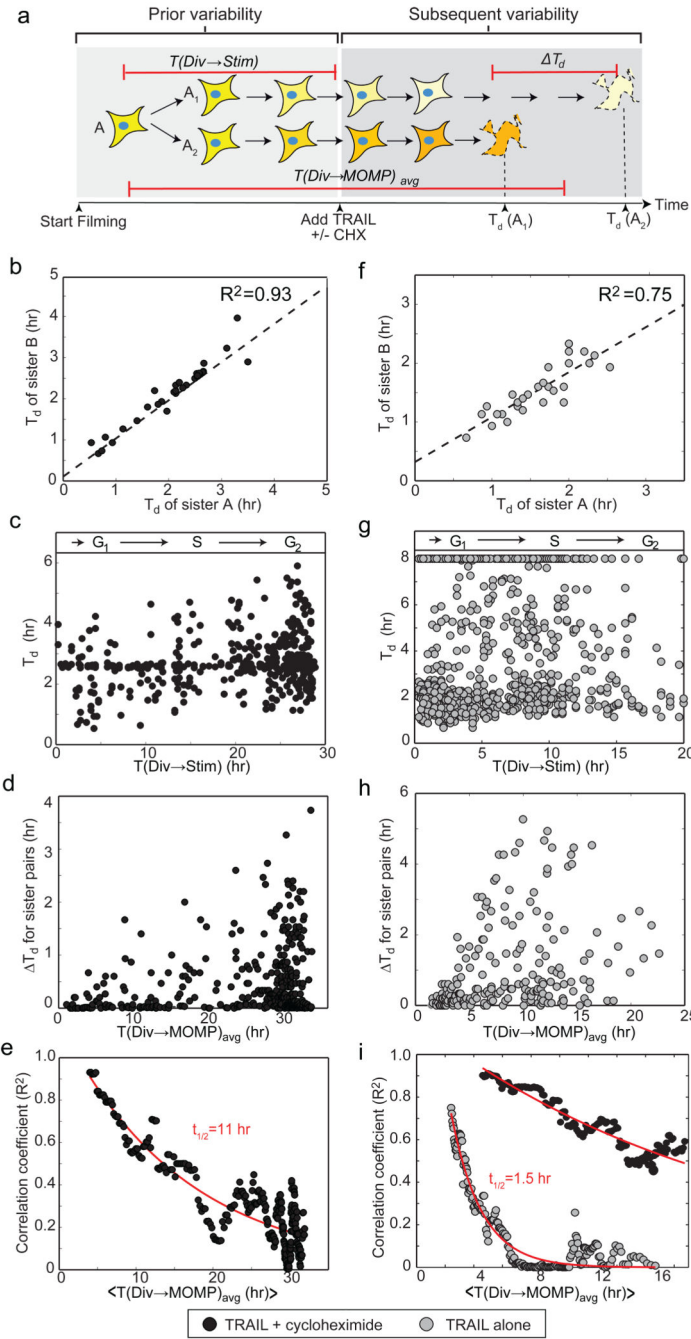
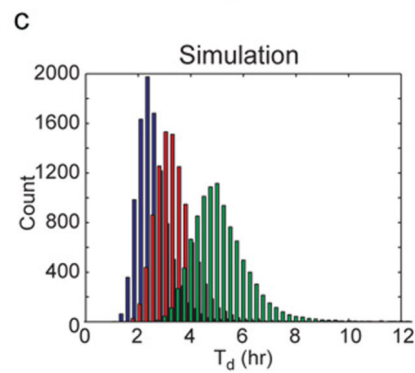
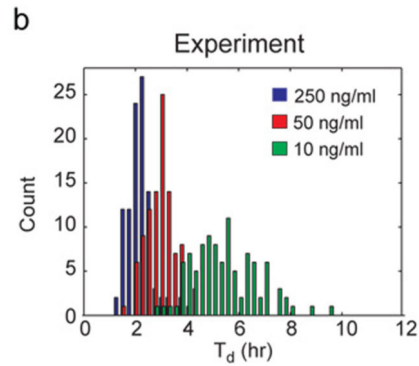
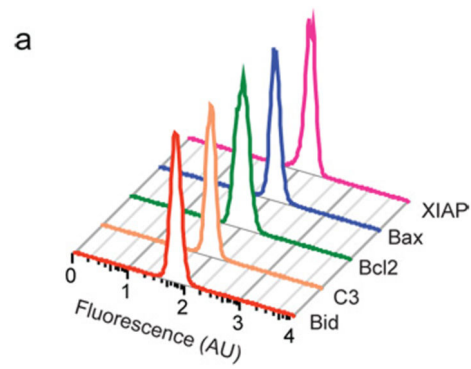


Figure 1. Time-to-death is highly correlated between HeLa sister cells but correlation decays as a function of time since division

a. Schematic of experimental design. T_d represents the difference in time of MOMP between sisters; $T(Div \rightarrow MOMP)_{avg}$ the time between cytokinesis of the mother and the average time of MOMP in daughter cells; $T(Div \rightarrow Stim)$ the time between cytokinesis and TRAIL addition. The shading of each cell depicts concentrations/states of relevant proteins. **b** and **f**, Similarity in T_d among pairs of recently divided sister cells ($T(Div \rightarrow MOMP)_{avg} < 7$ hr for (b) and < 3.5 hr for (f)). **c** and **g**, T_d as a function of $T(Div \rightarrow Stim)$, a proxy for cell

cycle state ($R^2 < 0.03$). **d** and **h**, T_d as a function of $T(Div \rightarrow MOMP)_{avg}$. **e** and **i**, Decay in the correlation of T_d between sister pairs as a function of $T(Div \rightarrow MOMP)_{avg}$. In (i), black circles represent data for cells treated with TRAIL plus cycloheximide imaged in parallel with the TRAIL alone treatment (Supplementary Fig. 5).



d Coefficients of variation in T_d

TRAIL dose	Experiment	Simulation
10 ng/ml	0.24	0.21
50 ng/ml	0.18	0.23
250 ng/ml	0.21	0.25

Figure 2. Endogenous variation in the concentrations of apoptotic regulators is sufficient to explain variability in T_d

a, Protein distributions in untreated HeLa cells determined by flow cytometry. **b** and **c**, Distributions of T_d for HeLa cells treated with TRAIL at concentrations indicated (with cycloheximide) as determined experimentally (**b**) or estimated by simulations (**c**). **d**, Coefficients of variation for distributions in (**b**) and (**c**).

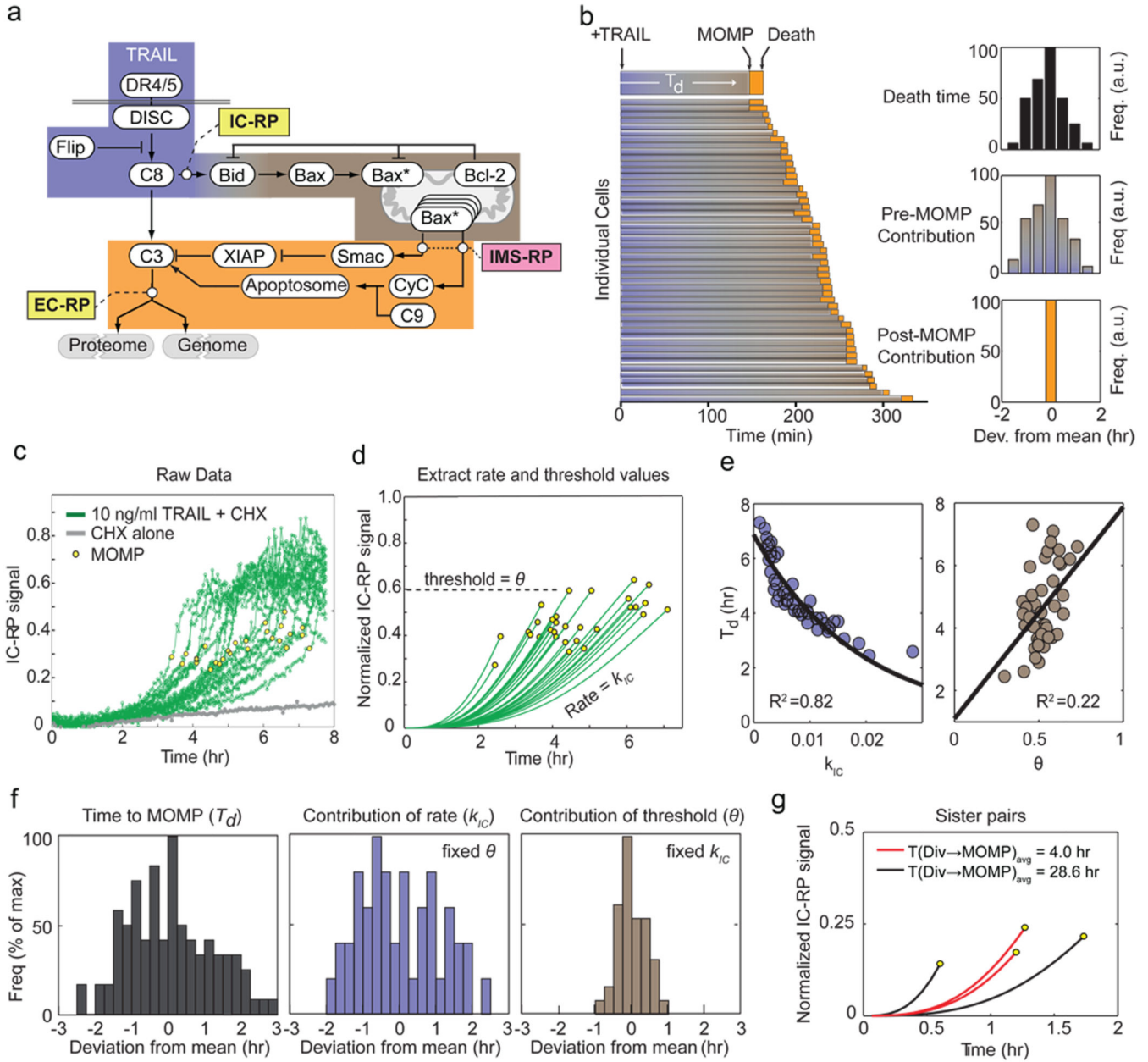


Figure 3. A single time-dependent process upstream of MOMP predicts time-to-death
a, Schematic of receptor-mediated apoptosis signalling with IC-RP, EC-RP, and IMS-RP indicated. The Bcl-2 protein family is represented in simplified form by Bid, Bax, and Bcl-2. Reactions occur before (blue), during (grey), or subsequent to MOMP (orange). **b**, Timing of apoptotic events in HeLa cells expressing IMS-RP and EC-RP and treated with TRAIL; blue-grey denotes the pre-MOMP interval and orange the interval between MOMP and half-maximal cleavage of EC-RP (a marker of death). Insets show death times computed from data (top) and contributions of pre-MOMP (middle) or post-MOMP (top) intervals. **c** and **d**, Raw and fitted trajectories for IC-RP cleavage in single TRAIL-treated HeLa cells co-expressing IMS-RP and IC-RP. Values for height of the MOMP threshold (θ) and rate of

approach to the threshold (k_{IC}) were derived by fitting (Supplementary Fig. 6). **e**, Correlation between T_d and k_{IC} (left) or θ (right) for data in (d). **f**, Relative contributions of variability in k_{IC} (blue) or θ (grey) to variability in T_d (black; Supplementary Fig. 7). **g**, Trajectories of IC-RP cleavage in recently divided sister HeLa cells having similar T_d (red) and older sisters with differing T_d (black) treated with 50 ng/ml TRAIL.

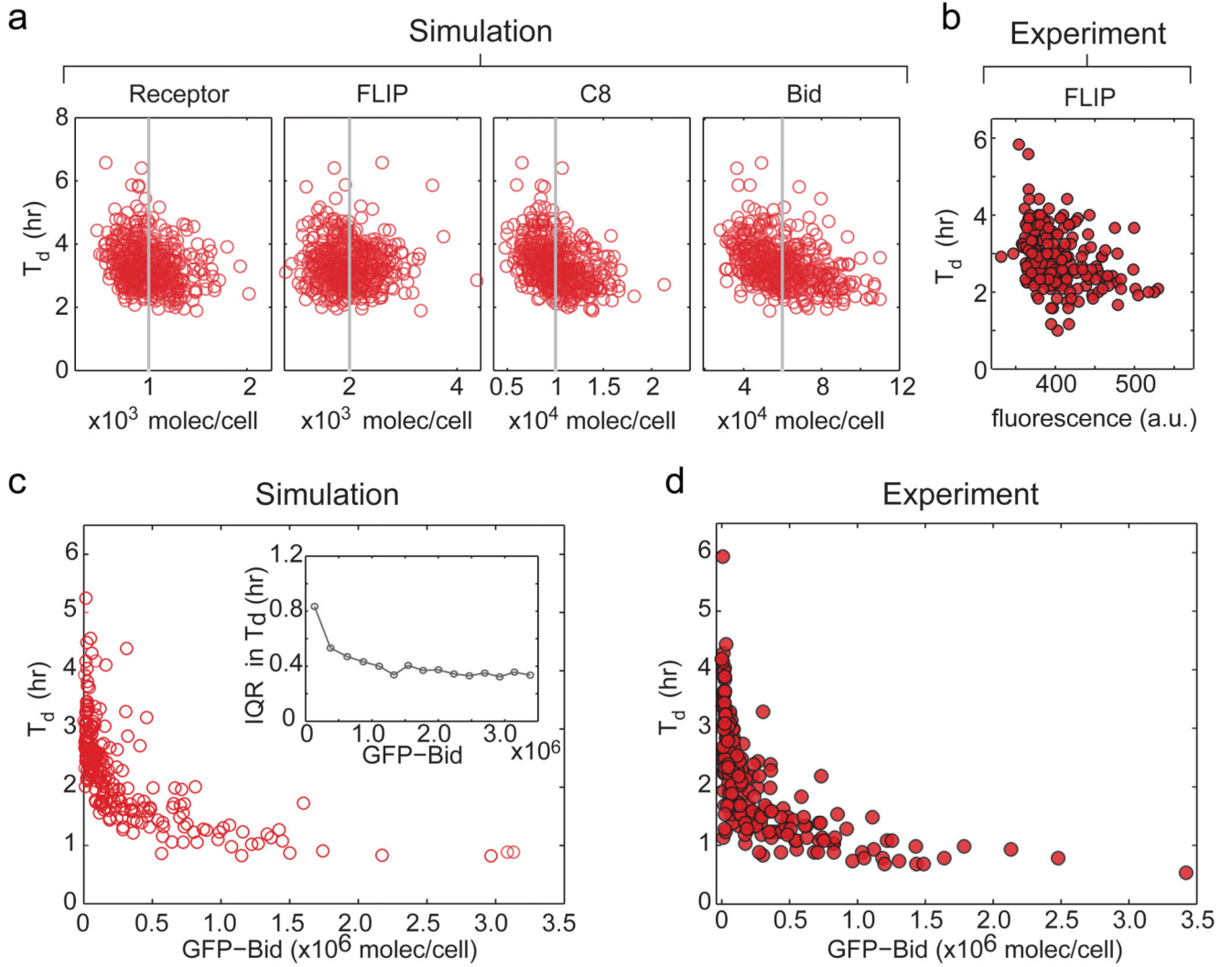


Figure 4. No single protein predicts T_d under normal conditions but over-expression can increase predictability

a, T_d as a function of four protein levels based on simulation. Grey lines denote mean protein concentration; each point represents a single simulated cell. **b**, Death time as a function of endogenous FLIP levels in H1299 cells. **c** and **d**, Effect of GFP-Bid over-expression on T_d in HeLa cells, as predicted by simulation (c) or observed in experiment (d). Inset shows reduction in dispersion of T_d with increasing Bid, as measured by interquartile range (IQR; Supplementary Fig. 8).